Scripta Materialia 134 (2017) 66–70

Contents lists available at ScienceDirect

Scripta Materialia

journal homepage: www.elsevier.com/locate/scriptamat

Regular article

Effects of cyclic heat treatment and aging on superelasticity in oligocrystalline Fe-Mn-Al-Ni shape memory alloy wires

H. Ozcan [a], Ji Ma [b], S.J. Wang [b], I. Karaman [a,b,*], Y. Chumlyakov [c], J. Brown [d], R.D. Noebe [e]

[a] Department of Mechanical Engineering, Texas A&M University, College Station, TX, USA
[b] Department of Materials Science and Engineering, Texas A&M University, College Station, TX, USA
[c] Siberian Physical Technical Institute, Tomsk 634050, Russia
[d] Dynalloy, Inc., Costa Mesa, CA, USA
[e] NASA Glenn Research Center, Cleveland, OH, USA

ARTICLE INFO

Article history:
Received 7 December 2016
Received in revised form 6 February 2017
Accepted 16 February 2017
Available online xxxx

Keywords:
Superelasticity
Martensitic transformation
Iron-based shape memory alloys
Stress induced martensite
Grain growth

ABSTRACT

The effects of nano-precipitation on stress-induced martensitic transformation (SIM) in $Fe_{43.5}Mn_{34}Al_{15}Ni_{7.5}$ shape memory alloy wires were investigated. It was shown that a large grain size to wire diameter ratio, i.e. an oligocrystalline structure, is necessary to obtain superelasticity. The critical stress for SIM and tensile strength at room temperature increase with aging time at 200 °C without loss of superelasticity. A superelastic strain of 6.7%, with tunable transformation stress level as high as 600 MPa, and a low stress hysteresis, was obtained in the aged wires.

Shape memory alloys (SMAs) are unique class of materials that display large reversible shape changes upon mechanical loading/unloading, i.e. superelasticity, enabled by a stress-induced martensitic transformation. NiTi alloys are the most well-known SMAs, which can exhibit up to 10% superelastic strain. They demonstrate reasonable ductility and relatively low elastic anisotropy [1,2]. However, they are difficult to cold work due to their ordered intermetallic structure [3]. In addition, they are highly composition-sensitive on the nickel-rich side of the stoichiometry, where 0.1 at% change in composition leads to a 20 °C change in transformation temperatures [4]. Besides the high cost of initial materials, difficulty of processing and the need to precisely control the chemistry further increases the cost and hinders the widespread use of NiTi.

Disordered Fe-based SMAs are alternatives to NiTi due to their inexpensive constituents and ease of processing. Since 1970s, many attempts have been made to develop Fe-based SMAs. However, only a few were successful in achieving superelasticity at room temperature. Maki et al. [5] were able to show reversible martensitic transformation by ausaging an FeNiCoTi alloy to form fine precipitates, however, they observed superelasticity only at −100 °C. A major breakthrough came in 2010, in the form of a polycrystalline FeNiCoAlTaB alloy [6]. This material exhibits room temperature superelasticity of up to 13.5% strain, but requires a strong [100] texture, coherent nano-precipitates, and large grain size to achieve superelasticity. In 2011, a new FeMnAlNi alloy was developed [7] that exhibits 5% room temperature superelasticity, but its performance is also dependent on nano-precipitates and large grain size. In single crystalline FeMnAlNi alloys, the effects of aging on the superelastic properties were studied by Tseng et al. [8]. They found that superelasticity, recoverable strain level, and stress hysteresis are controlled by the size of the precipitates. A unique feature of this alloy is a small temperature dependence of the critical stress for stress-induced martensitic transformation (σ_{SIM}) of 0.41 MPa/°C, which is almost 15 times smaller than that of NiTi [9]. This characteristic is crucial for structural and civil infrastructure applications that require a stable superelastic response over a broad temperature range.

Fe-based SMAs, on the other hand, usually suffer from large elastic and transformation strain anisotropy similar to Cu-based SMAs [10–13]. This leads to high internal stresses at grain boundaries between grains with large orientation mismatches upon martensitic transformation [11,14]. Additionally, most of the Fe-based SMAs have a limited number of martensite variants [15]. Therefore, strain accommodation at grain boundaries during the transformation becomes more difficult

* Corresponding author at: Department of Mechanical Engineering, Texas A&M University, College Station, TX, USA.
E-mail address: ikaraman@tamu.edu (I. Karaman).

http://dx.doi.org/10.1016/j.scriptamat.2017.02.023
1359-6462/

and, together with high stresses, causes intergranular fracture and/or a suppression of superelastic behavior [11,14,16].

Thus, to obtain good superelasticity, it is necessary to decrease the total grain boundary area and triple junctions, and limit the effect of grain boundary constraint during the transformation [7,17–19]. Ueland et al. [17,18,20] and Chen et al. [21] produced bamboo structured microwires and obtained 7% superelasticity in Cu-Al-Ni microwires. Similarly, in Fe-based SMAs, it has been shown that grain size to wire diameter (d/D) [19] or grain size to sheet thickness ratios larger than one [7] is a necessary condition to obtain superelasticity.

Techniques to obtain large grain size through abnormal grain growth in FeMnAlNi SMAs involve cyclic heat treatments where samples are repeatedly cycled between the single phase and two phase regions in the phase diagram. Omori et al. [19] annealed FeMnAlNi wires and sheets at 1200 °C followed by air cooling, and repeated this process until they obtained large grain size. Vollmer et al. [16] have applied similar cyclic heat treatments, cycled between 1200 °C and 900 °C and obtained coarse grains in the FeMnAlNi flat, thin tension specimens.

A few studies on FeMnAlNi polycrystals have recently focused on suppressing intergranular fracture [16,19] and investigating the effect of grain size on superelastic behavior. Additionally, it has been shown that various aging treatments on FeMnAlNi single crystals improve the mechanical response and superelastic behavior [9]. However, the latter has not been studied in polycrystalline/oligocrystalline FeMnAlNi SMAs. In the present work, we investigate the effect of post-cyclic heat treatment and nano-precipitation on the superelastic behavior and mechanical properties of FeMnAlNi polycrystalline wires.

Ingots with a nominal composition of Fe-34%Mn-15%Al-7.5%Ni (at%) were prepared by vacuum induction melting. To enable wire drawing of the FeMnAlNi at room temperature it is necessary to create a two-phase microstructure consisting of a bcc alloy matrix containing ductile fcc second phase. To generate this microstructure, the ingots were first hot extruded at 1000 °C with an area reduction ratio of 7:1. The resulting rods were then solution treated at 1200 °C and annealed at 900 °C for 30 min under high purity argon followed by a water quench (Fig. 1a). The 900 °C treatment was performed to introduce the high volume fraction of ductile second phase particles necessary for wire drawing. The heat treated rod was then cold-drawn into wire with a final diameter of 0.5 mm, following an area reduction of 75%. Final chemical composition of the wires was determined using Wavelength Dispersive Spectroscopy (WDS) and compositional variations were found to be less than 0.2 at% from the nominal.

To promote abnormal grain growth, the wires were encapsulated in quartz tubes, evacuated, and filled with high-purity argon and then subjected to cyclic heat treatments. The encapsulated wires were cycled five times between the single phase region (1200 °C) and room temperature, by placing the encapsulated wires in a pre-heated furnace for 0.5 h and removing them from the furnace and cooling to room temperature in air. After these steps, the encapsulated wires were solution heat treated (SHT) at 1300 °C for 30 min and quenched in water. Finally, nano-sized precipitates were formed with precipitation heat treatments at 200 °C for 1, 3, 5 and 24 h.

Microstructure of the wires was investigated using a Keyence digital microscope. Specimens for optical microscopy were prepared by

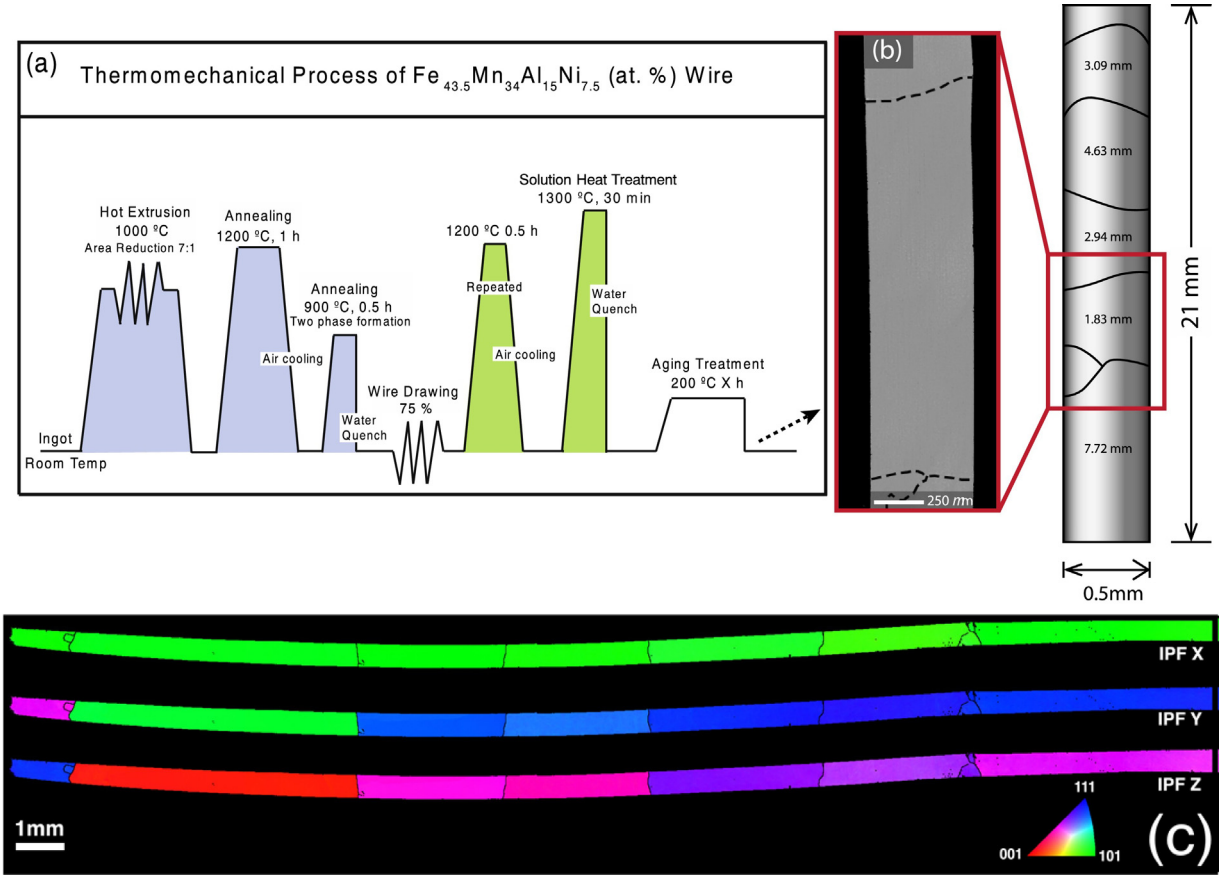

Fig. 1. (a) Thermomechanical processing history of Fe-34%Mn-15%Al-7.5%Ni (at%) superelastic wire. (b) Final grain sizes and distribution in a representative Fe-34%Mn-25%Al-7.5%Ni (at%) superelastic wire after cyclic grain growth treatment and final solution heat treatment at 1300 °C for 30 min (as defined in (a)). (c) EBSD orientation mapping of a $Fe_{43.5}Mn_{34}Al_{15}Ni_{7.5}$ (at%) wire aged at 200 °C for 24 h after tensile superelastic test (the superelastic response is shown in Fig. 3c). The colors represent the crystal directions parallel to the drawing direction (IPFX), the transverse direction (IPFY) and the normal direction (IPFZ), given in the stereographic triangle. (For interpretation of the references to color in this figure legend, the reader is referred to the web version of this article.)

mechanical grinding and polishing through 0.25 μm diamond paste followed by a final polish using 0.04 μm colloidal silica. Finally, samples were etched using a solution of 4% nitric acid and 96% ethanol by volume. Transmission electron microscopy (TEM) samples were prepared by twin-jet electro-polishing with a solution of 30% nitric acid and 70% methanol by volume at −20 °C. TEM investigations were conducted using a FEI Tecnai G^2 F20 electron microscope. Crystallographic texture was measured using electron backscatter diffraction (EBSD) technique conducted at room temperature on a Tescan FERA-3 scanning electron microscope (SEM) with an accelerating voltage of 20 kV. EBSD samples were prepared identically to those for optical microscopy.

To promote superelasticity in these alloys, the grain size to wire diameter ratio must be larger than 1 [19]. The final grain sizes and distribution in a representative wire are shown in Fig. 1b where the oligocrystalline wire with bamboo structured grains can be seen. The grains have a large average d/D ratio of ~8. The microstructure contains a small number of triple junctions and the number density of grain boundaries is small. The majority of the grain boundaries are perpendicular to the wire axis and span the cross section of the wire. Fig.1c shows that FeMnAlNi wire possesses strong [110] texture in the drawing direction after cyclic abnormal grain growth followed by solution heat treatment.

In addition to large grains, nano-sized B2 precipitates (as evidenced in the selected area diffraction pattern in Fig. 2c) are also prerequisite for superelasticity in FeMnAlNi. The volume fraction and size of the precipitates greatly influence the superelastic characteristics, such as transformation stress levels, transformation temperatures, martensite morphology, and hysteresis [8,10]. High resolution TEM images in Fig. 2a and b show the average precipitate sizes after aging at 200 °C for 1 h and 3 h to be 4–6 nm and 6–9 nm, respectively.

Uniaxial tensile tests were performed at room temperature using an electro-mechanical MTS load-frame to characterize the superelastic response. Tensile strain was measured with an MTS LX1500 laser extensometer with laser tags directly attached to the wire. Gage length of the wires was 50 mm. Specimens were deformed at a nominal strain rate of $5 \times 10^{-4}\ s^{-1}$, first to 0.5% strain, unloaded, then loaded again to 1% and unloaded. Following this procedure, the applied strain level was increased in 1% increments and the specimens were tested until failure. These incremental strain experiments were utilized to investigate the effect of aging condition on the stress induced martensitic transformation. From these incremental tests, superelastic properties of the wires, such as critical stress for SIM (σ_{SIM}), stress hysteresis, superelastic strain (σ_{SE}), elastic strain (σ_E), and irrecoverable strain (σ_{irrec}) were determined.

Fig. 3a–c show the stress-strain response of $Fe_{43.5}Mn_{34}Al_{15}Ni_{7.5}$ wires at room temperature after aging at 200 °C for (a) 1 h, (b) 3 h and (c) 24 h. σ_{SIM}, determined from the first loading cycles, are plotted in Fig. 3d as a function of increasing aging time at 200 °C. The σ_{SIM} level increases monotonically with increasing aging time for short duration aging, plateauing around 600 MPa for aging treatments longer than 5 h. The increase in transformation stress is attributed to a decrease in transformation temperatures, which are dependent on the size of the precipitates and the composition change in the matrix upon precipitation [8].

Previous studies on rolled polycrystalline sheets with similar aging treatments demonstrated maximum transformation stress levels around 200 MPa [7], which is significantly lower than 600 MPa observed here. It has been reported that a random texture is developed after cold rolling in these alloys [7]. Wire drawing, on the other hand, results in a [110] texture after 75% cold work as shown in the Fig. 1c, and a similar [110] texture was also reported by Omori et al. in FeMnAlNi wires [19]. Since both sample forms have bamboo structured grains, overall deformation properties of both materials are expected to be highly dependent on individual grain orientations leading to different σ_{SIM} values even though they are aged under the same conditions.

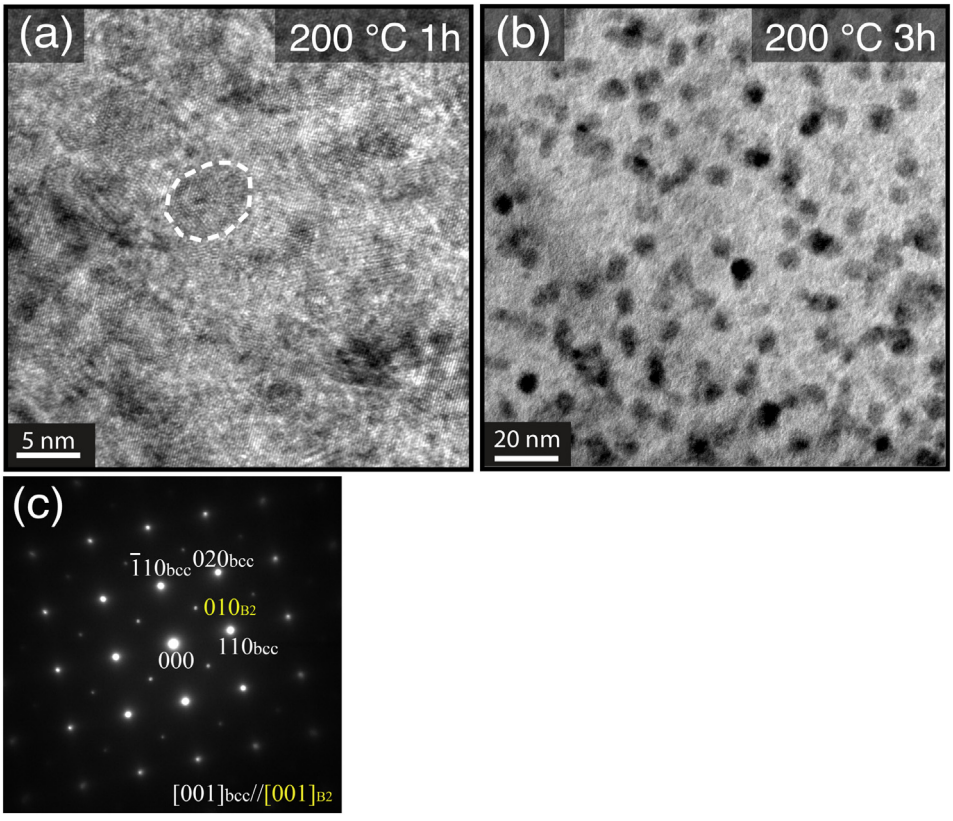

Fig. 2. Microstructure of the Fe-34%Mn-15%Al-7.5%Ni (at%) alloy; (a) high resolution TEM image showing B2 precipitates after aging at 200 °C for 1 h. (b) Conventional TEM image of the B2 precipitates after aging at 200 °C for 3 h. (c) Selected area diffraction pattern of a single BCC matrix grain oriented along the [001] direction after solution heat treatment [8].

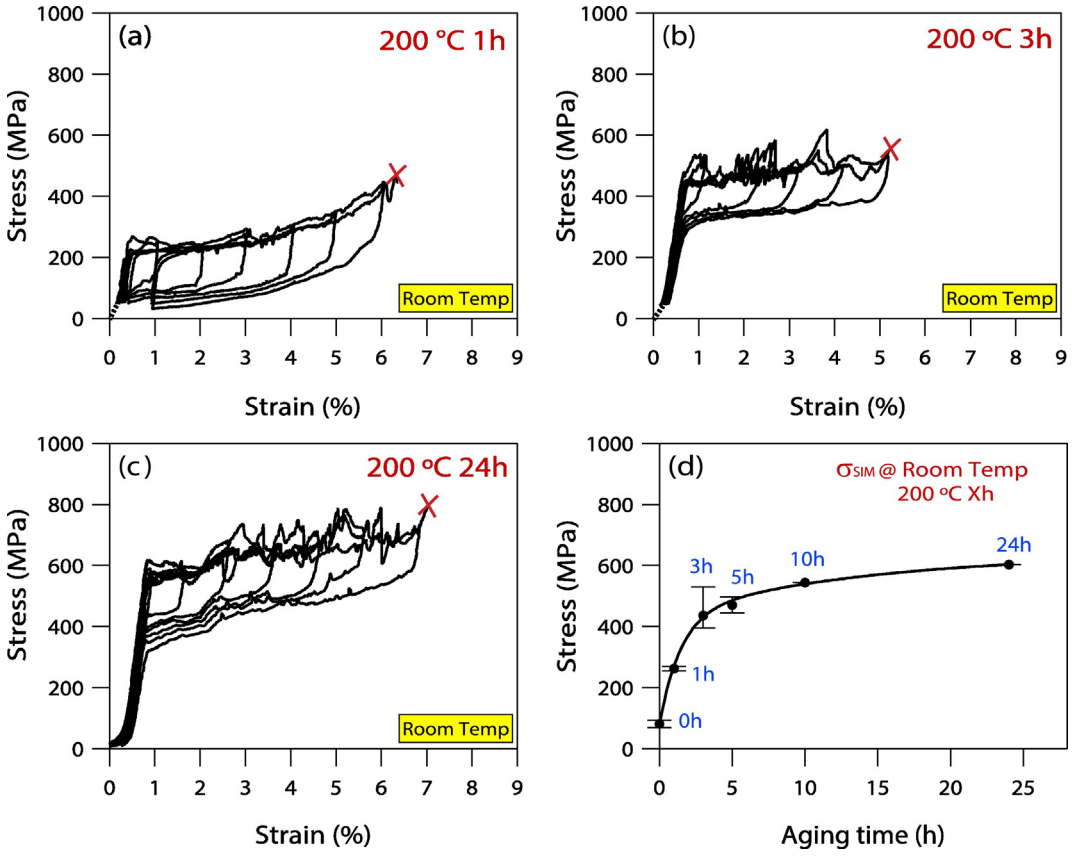

Fig. 3. Room temperature tensile superelastic responses of Fe-34%Mn-15%Al-7.5%Ni (at%) wire subjected to the cyclic abnormal grain growth method, followed by solution heat treatment at 1300 °C, and aging at 200 °C for (a) 1 h (b) 3 h and (c) 24 h. (d) Summary of the critical stress for stress induced martensitic transformation (σ_{SIM}) versus aging time of the Fe-34%Mn-15%Al-7.5%Ni (at%) wires after cyclic abnormal grain growth and aging at 200 °C.

In superelasticity tests, the stress hysteresis is defined as the difference between the stress levels for stress-induced forward and reverse martensitic transformations during loading and unloading, respectively. This is a measure of energy dissipation during transformation. To investigate the effect of nano-precipitates on stress hysteresis, the stress hysteresis at 3% applied strain is plotted as a function of increasing aging time in Fig. 4a. Clearly, the stress hysteresis decreases with aging time from 1 h to 3 h, but after 3 h it increases monotonically. The decrease in stress hysteresis during aging from 1 to 3 h was also previously observed in FeMnAlNi single crystals oriented along the <001> direction [8]. In this study, the 200 °C 3 h heat treatment was reported to be the peak aging condition where the best superelastic response was observed [8]. In both the single crystalline and oligocrystalline materials, coherent precipitates lower the hysteresis and improves recoverability. Compared to aging for 3 h, the observation of irrecoverable strain in the 200 °C/1 h aged sample after 5% strain (Fig. 3a) indicates that matrix strength is not sufficient to prevent dislocation generation during transformation, which in turn increases energy dissipation.

After aging for times longer than 3 h we observe an increase in the stress hysteresis. This is due to higher frictional resistance to interfacial motion in the matrix due to the coarsening of precipitates [8,22], leading to higher energy dissipation. At a given aging condition, the hysteresis generally increases with applied strain level (Fig.4b), which is expected due to a larger transforming volume fraction of austenite and greater energy dissipation due to martensite variant-variant interactions [23]. The decrease in hysteresis between 2 and 3% applied strains is likely caused by the training effect due to the initial superelastic increments. With a proper aging time and temperature

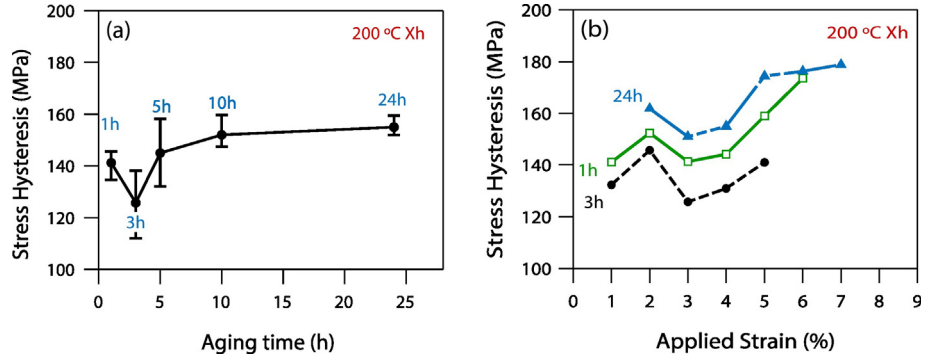

Fig. 4. Stress hysteresis of Fe-34%Mn-15%Al-7.5%Ni (at%) wires during superelastic experiments. (a) Change of stress hysteresis with aging time at 200 °C. Stress hysteresis is calculated at 3% applied strain in each aging condition. (b) The relationship between the stress hysteresis and the applied strain level for three different aging conditions.

(200 °C 24 h) it is shown here that FeMnAlNi wires can transform and recover up to 6.7% strain with a critical stress level of 600 MPa. This strength level with low hysteresis has not been previously reported in polycrystalline FeMnAlNi superelastic wires or sheets.

In all aging conditions studied here, the strain level at fracture does not change notably during the incremental strain experiments, and the average value is about 7%. The maximum recoverable strain for each case is mostly dictated by the failure of the samples. Therefore, it is not possible to conclude how aging time affects the maximum recoverable strain levels. Fig. 3b and c show that samples failed at 6 to 7% strain level while transformation is still in the first plateau region before the onset of hardening. This also suggests that the stress induced phase transformation may not be fully complete. Local stress concentrations near grain boundaries due to the martensite reorientation and detwinning, and in particular at the few triple junctions that exist in the samples, are responsible for failure.

The superelastic stress-strain curves in Fig. 3a–c show serrated response, which is more pronounced during the forward transformation. Similar serrated stress strain behaviors were observed previously in other FeMnAlNi alloys and in magnetic SMAs such as NiMnGa [24,25]. Omori et al. reported serrated stress-strain behavior in FeMnAlNi polycrystalline wires with a d/D ratio greater than one [19]. They also observed that serrations increased as the grain size to diameter ratio increased. These serrations were attributed to the nucleation barriers for martensitic transformation. Vollmer et al. [16] observed similar behavior in FeMnAlNi polycrystalline rolled tension samples. They were able to link each stress drop to the transformation of a single oligocrystalline grain into a single variant martensite [16]. However, in the present study, we only observe pronounced serrations in the samples that are aged at 200 °C for 3 h and longer. Serrated flow, while present in samples aged at 200 °C for 1 h, was much finer in scale and less pronounced despite the large oligocrystalline grains (the d/D ratio was higher than 8). Therefore, the size of the nano-precipitates seems to have an effect on the serrated flow behavior in these materials.

Serrated deformation behavior has also been observed in NiMnGa [24,25], however the serrations were linked to the surface roughness of the samples. The damaged surface layer resulting from spark plasma cutting or introduced via surface preparation can become stress concentrators, acting as finely dispersed pinning sites for twin boundaries, and limits the ability of the martensite to coarsen. When the surface damage is removed, the twin boundaries rapidly propagate until they are stopped by the defects within the matrix and the twins become coarser [24]. Each pinning event results in a small stress increase and stress relaxation; however, this stress change is usually small as compared to what is observed for the FeMnNiAl samples aged 3 h and longer. Therefore, in the present case, the large stress drops are believed to be related to the transformation of an individual austenite grain to a single variant martensite. Small stress drops are likely to be influenced by the surface roughness of the wires. When the nano-precipitates are small and the matrix is relatively soft, the martensite phase front propagates continuously leading to smoother stress-strain response.

The major findings can be summarized as follows:

(1) The superelastic properties of FeMnAlNi oligocrystalline wires, such as transformation stress and hysteresis, are highly dependent on the volume fraction and size of nano-precipitates. As the aging time increases, the transformation stress increases, while the hysteresis can increase or decrease depending on the aging time.

(2) Aging at 200 °C for 24 h results in a 600 MPa transformation stress with a fully recoverable superelastic strain up to 6.7%. This recoverable strain with high strength levels has not been previously reported in FeMnAlNi polycrystalline samples and they are on par with those observed in commercial NiTi shape memory alloy wires.

Acknowledgements

This work was supported by National Science Foundation — International Materials Institute Program through the Grant No DMR 08-44082, Office of Specific Programs, Division of Materials Research, Arlington, Virginia. RDN gratefully acknowledges support from the NASA Transformative Aeronautics Concepts Program, Transformational Tools & Technologies Project.

References

[1] K. Otsuka, C.M.C.M. Wayman, Shape Memory Materials, Cambridge University Press, 1999.
[2] K. Otsuka, X. Ren, Prog. Mater. Sci. 50 (2005) 511–678.
[3] T. Tadaki, C.M. Wayman, Scr. Metall. 14 (1980) 911–914.
[4] J. Frenzel, E.P. George, A. Dlouhy, C. Somsen, M.F.X. Wagner, G. Eggeler, Acta Mater. 58 (2010) 3444–3458.
[5] T. Maki, K. Kobayashi, M. Minato, I. Tamura, Scr. Metall. 18 (1984) 1105–1109.
[6] Y. Tanaka, Y. Himuro, R. Kainuma, Y. Sutou, T. Omori, K. Ishida, Science 327 (2010) 1488–1490.
[7] T. Omori, K. Ando, M. Okano, X. Xu, Y. Tanaka, I. Ohnuma, R. Kainuma, K. Ishida, Science 333 (2011) 68–71.
[8] L.W. Tseng, J. Ma, B.C. Hornbuckle, I. Karaman, G.B. Thompson, Z.P. Luo, Y.I. Chumlyakov, Acta Mater. 97 (2015) 234–244.
[9] L.W. Tseng, J. Ma, S.J. Wang, I. Karaman, M. Kaya, Z.P. Luo, Y.I. Chumlyakov, Acta Mater. 89 (2015) 374–383.
[10] J. Ma, B.C. Hornbuckle, I. Karaman, G.B. Thompson, Z.P. Luo, Y.I. Chumlyakov, Acta Mater. 61 (2013) 3445–3455.
[11] S. Miyazaki, T. Kawai, K. Otsuka, J. Phys. Colloq. 43 (1982) 813–818.
[12] J.L. Liu, H.Y. Huang, J.X. Xie, Mater. Des. 64 (2014) 427–433.
[13] L.W. Tseng, J. Ma, S.J. Wang, I. Karaman, Y.I. Chumlyakov, Scr. Mater. 116 (2016) 147–151.
[14] S. Miyazaki, T. Kawai, K. Otsuka, Scr. Metall. 16 (1982) 431–436.
[15] J. Ma, B. Kockar, A. Evirgen, I. Karaman, Z.P. Luo, Y.I. Chumlyakov, Acta Mater. 60 (2012) 2186–2195.
[16] M. Vollmer, C. Segel, P. Krooß, J. Günther, L.W. Tseng, I. Karaman, A. Weidner, H. Biermann, T. Niendorf, Scr. Mater. 108 (2015) 23–26.
[17] S.M. Ueland, C.A. Schuh, J. Appl. Phys. 114 (2013) 53503.
[18] S.M. Ueland, Y. Chen, C.A. Schuh, Adv. Funct. Mater. 22 (2012) 2094–2099.
[19] T. Omori, M. Okano, R. Kainuma, APL Mater. 1 (2013) 32103.
[20] S.M. Ueland, C.A. Schuh, Acta Mater. 60 (2012) 282–292.
[21] Y. Chen, X. Zhang, D.C. Dunand, C.A. Schuh, Appl. Phys. Lett. 95 (2009) 171906.
[22] R.F. Hamilton, H. Sehitoglu, Y. Chumlyakov, H.J. Maier, Acta Mater. 52 (2004) 3383–3402.
[23] M. Vollmer, P. Krooß, M.J. Kriegel, V. Klemm, C. Somsen, H. Ozcan, I. Karaman, A. Weidner, D. Rafaja, H. Biermann, T. Niendorf, Scr. Mater. 114 (2016) 156–160.
[24] M. Chmielus, K. Rolfs, R. Wimpory, W. Reimers, P. Müllner, R. Schneider, Acta Mater. 58 (2010) 3952–3962.
[25] M. Chmielus, P. Müllner, Mater. Sci. Forum 684 (2011) 175–199.